JOURNAL OF SOLID STATE CHEMISTRY 85, 251–261 (1990)

Point Defects and Ion Migration in PbFCl

M. S. ISLAM*

Corporate Research Laboratories, Eastman Kodak Company, Rochester, New York 14650-2021

Received July 31, 1989; in revised form December 5, 1989

Atomistic simulation techniques have been applied to PbFCl in order to calculate the energetics of defect formation and ion transport mechanisms in the undoped material. Schottky-like disorder is computed to be the dominant ionic defect. The activation energies for a variety of anion vacancy migration mechanisms are calculated and found to be in good agreement with experiment. The results support the models in which the low temperature ionic conductivity is attributed to an interplanar Cl vacancy mechanism. We predict that the out-of-plane configuration of the Cl_2^- species is the most stable self-trapped hole (V_k center). Interatomic separations of the V_k centers following lattice relaxation are also discussed.

1. Introduction

Lead fluorochloride has been the subject of a number of experimental studies concerned with optical (*1–4*), photoconductivity (*5*), and ionic conductivity (*6–8*) measurements of the pure and doped material. From the conductivity studies it has been established that the dominant intrinsic defect is of the Schottky type and that both anions are mobile. Interestingly, it was previously assumed, by analogy with cubic PbF_2, that anion-Frenkel disorder would be the more favorable defect (*9*). PbFCl crystallizes into a tetragonal layered structure (space group $P4/nmm$, D_{4h}^7) which consists of planes perpendicular to the c-axis (*10*); the most interesting structural feature is the existence of two adjacent planes of chloride ions. Indeed, the relatively easy cleavage along the (001) plane is associated with the weak bonding between these two planes. The Pb and F sublattice is related to the fluorite structure of PbF_2, but the space available for interstitial ions is much reduced. The layered nature of the structure suggests that anisotropic electrical properties are expected and are in fact exhibited (*6–8*). It is worth noting that this low-symmetry structure is the prototype for important classes of materials, such as BaFX and LaOX (where $X \equiv$ Cl, Br), that have received considerable scientific and technological interest due to their luminescence properties and X-ray imaging applications (see, e.g., Refs. (*11–14*)).

Despite the range of experimental studies of PbFCl, there are still several problems with our understanding of this material. First, the precise nature of the ion transport properties has not been unambiguously established due to the presence of several possible migration mechanisms. Second,

* Present address: Department of Chemistry, University of Surrey, Guildford, Surrey GU2 5XH, UK.

0022-4596/90 $3.00

although information is available on ionic defects in the pure material, the energetics of formation and defect configurations of hole centers have not been investigated. The latter defects, which include the self-trapped hole or V_k center, have been previously discussed in connection with the alkali halides and are of particular importance in relation to mechanisms of photostimulated luminescence. In addition, the difficulty of obtaining pure crystals for investigation, due to either deviation from the molecular composition owing to excess halide ion content or the possibility of oxygen impurities (*1, 4, 5, 7*), has caused problems in the interpretation of experimental results.

The aim of the present study is to further elucidate the defect structure of PbFCl by the application of atomistic computer simulation techniques. The reliability of such theoretical techniques for calculating defect and migration energies in solid state materials has been demonstrated by several studies on alkali halides (*15–17*), alkaline–earth halides (*16, 18, 19*), and most recently alkaline–earth fluorohalides (*20, 21*). Our calculations include the formation energies of localized defects and the migration activation energies for anion vacancy species, in relation to undoped PbFCl. Such defect simulations, a necessary prerequisite to the investigation of more complex defect models in the doped material, have so far not been presented for PbFCl.

2. Methodology and Potentials

The defect simulations are performed using theoretical methods based on the generalized Mott–Littleton procedure for noncubic crystals, incorporated in the HADES (*22*) and CASCADE (*23*) computer codes. More detailed reviews of these methods and applications to other systems are given by Catlow and Mackrodt (*24*) and Agullo-Lopez *et al.* (*25*). An important feature of the defect calculations is the treatment of lattice relaxation about the defect. The Mott–Littleton approach divides the crystal into two regions so that the ion–ion interactions in the inner region (I), immediately surrounding the defect, are treated explicitly while the ions in the remainder of the crystal are relaxed by continuum methods. For the results presented here 200 ions were used in region I, which is sufficiently large for the calculated energy to be no longer sensitive to additional expansion of the region. Previous simulation studies have shown that, with a large enough region I, the accuracy of the calculations is primarily determined by the lattice potentials describing the interatomic interactions. These are typically described by fully ionic, pairwise potentials of the form

$$\phi_{ij} = \frac{Z_i Z_j e^2}{r_{ij}} + A_{ij} \exp(-r_{ij}/\rho_{ij}) - C_{ij}/r_{ij}^6 \quad (1)$$

which consists of the usual long-range Coulomb term and a Born–Mayer representation of the overlap repulsion between the ions, supplemented by a van der Waals attractive term. Note that the $1/r$ summation is slowly convergent when handled in real space and is, therefore, treated by the Ewald method, which involves a transformation into reciprocal space. The potentials also incorporate the shell model (*26*) to describe both ionic polarization and the effect that the polarization has in modifying the effective overlap interactions.

The short-range potential parameters assigned to each ion–ion interaction were derived empirically by a least-squares fitting routine to minimize the strains acting on the ions within the unit cell (i.e., internal basis strains) and on the unit cell as a whole (i.e., bulk lattice strains). The starting potentials were either transferred directly from previous simulation studies of BaFCl (*20*) and PbF_2 (*27*) for the relevant anion–anion and Pb–F interactions, respectively, or com-

TABLE I

INTERATOMIC POTENTIALS

(a) PbFCl lattice

(i) Short range: $V(r) = A \exp(-r/\rho) - C/r^6$

Interaction	A (eV)	ρ (Å)	C (eV Å^6)
Pb^{2+}–Pb^{2+}	81,035.5	0.1003	79.1
Pb^{2+}–F^-	2,973.1	0.2833	0.0
Pb^{2+}–Cl^-	2,381.9	0.3373	0.0
F^-–F^-	2,008.6	0.1937	67.5
F^-–Cl^-	556.83	0.3707	48.8
Cl^-–Cl^-	9,909.3	0.3112	183.5

(ii) Shell model[a]

Species	Y(e)	k (eV Å^{-2})
Pb^{2+}	−4.559	297.9
F^-	−2.390	204.6
Cl^-	−2.515	188.2

(b) X_2^- molecule[b]

(i) Short range: $V(r) = A \exp(-r/\rho) - C/r^6$

Interaction	A (eV)	ρ (Å)	C (eV Å^6)
F_2^-	17,279.0	0.2366	343.2
Cl_2^-	11,956.7	0.3339	1913.7

(ii) Shell model[a]

Species	Y(e)	k (eV Å^{-2})
$F^{-1/2}$	−2.390	204.6
$Cl^{-1/2}$	−2.485	54.2

[a] Y and k refer to shell charge and harmonic force constant, respectively.

[b] From Refs. (*36, 37*).

puted using the electron–gas method (*16, 28*) for the Pb–Pb and Pb–Cl repulsive interactions. The resulting potentials and shell model parameters are listed in Table I. We should add that the empirical procedure for parameter derivation gives a good representation of the potential at or near equilibrium interatomic separations. However, for certain defect configurations, such as interstitials, where the interatomic separations may deviate from the normal lattice values, the validity of the analytical form representing the potential is assumed, which is open to question. Despite this reservation, numerous studies using empirical potentials have successfully calculated defect migration energies in which ions are displaced from perfect lattice positions. An extensive discussion of interatomic potentials as applied to ionic solids is given by Stoneham and Harding (*29*).

Prior to carrying out the defect simulations, the cell dimensions and all the ion positions in the unit cell are equilibrated (i.e., relaxed under constant pressure conditions), which corresponds to zero internal and bulk lattice strain. The magnitudes of the ion displacements from the observed crystal lattice positions to the equilibrated positions are small. Table II shows the comparison between the calculated and experimental bond lengths; the deviation is generally small with the largest discrepancy less than 0.06 Å. This clearly shows that the potentials for PbFCl produce an equilibrium structure which is close to that observed experimentally. Ideally, additional crystal properties, particularly dielectric and elastic constants and phonon spectra, are required to assess the potential model in greater detail. Such experimental data would also allow the potentials to be refined by further fitting. Despite the lack of data

TABLE II

CALCULATED AND EXPERIMENTAL BOND LENGTHS (IN Å)

Bond[a]	r (exp)	r (calc)	Δ
Pb–F	2.511	2.505	0.006
Pb–Cl^{I}	3.099	3.080	0.019
Pb–Cl^{II}	3.253	3.306	0.053
F–F	2.903	2.866	0.037
F–Cl^{I}	3.259	3.266	0.007
Cl^{I}–Cl^{II}	3.624	3.631	0.007

[a] Cl^{I} refers to the four Cl ions surrounding Pb at an equal distance, and Cl^{II} refers to the Cl ion directly above Pb, in the unit cell (shown in Fig. 2).

TABLE III

CALCULATED PROPERTIES OF THE PERFECT CRYSTAL

Property	PbFCl
Lattice energy (eV)	23.80
a (Å)	4.071 (4.106)[a]
c (Å)	7.321 (7.230)[a]
BLS[b]	0.0099
Elastic constants (10^{11} dyne/cm^2)	
C_{11}	10.01
C_{12}	2.16
C_{13}	4.01
C_{33}	7.03
C_{44}	3.46
C_{66}	2.33
Dielectric constants	
ε_0	8.78, 7.81
ε_∞	1.46, 1.44

[a] Observed values in parentheses.

[b] Mean bulk lattice strain after constant volume minimization.

for comparison, the calculated crystal properties, reported in Table III, are in accord with the observed values and general trends for the isostructural materials BaFCl and SrFCl (*30*). Furthermore, negative values for both the dielectric and elastic constants, which would indicate instabilities in the potential model, were not computed. The present results, therefore, provide support for the methods used and suggest that useful defect calculations can be performed with the present set of potentials for PbFCl.

3. Results and Discussion

3.1. Ionic Defects

We first calculated the energies of formation of isolated vacancies and interstitials (both cation and anion), which are given in Table IV. For vacancies the formation energy corresponds to removing a lattice ion from the perfect crystal to infinity; likewise, for interstitials the formation energy corresponds to introducing an ion from infinity into the perfect crystal. From examination of the anion vacancy energies it is clear that it is energetically more favorable to form vacancies in Cl^- rather than F^- positions. For the interstitial ions various sites in the unit cell are considered. The only stable position is found near the center of the face comprised of Pb and Cl ions. The final positions of the interstitials within this plane, following relaxation to a minimum energy configuration, are shown in Fig. 1. For all three interstitial ions, we find a small displacement off the center position, but only in the c-direction.

In addition to vacancies and interstitials, the formation energetics of antisite defects were investigated, i.e., replacing Cl^- by F^- and replacing F^- by Cl^-. The defect energies for these substitutional species are included in Table IV. Examination of the values reveals that replacing a Cl^- ion by an F^- ion is favorable, while the reverse process is highly unfavorable. This result is in accord with arguments based upon ion size, in which the small ion allows the lattice to relax around it, whereas the large ion causes a slight distortion in the local structure. We note that similar results have been

TABLE IV

CALCULATED FORMATION ENERGIES OF ISOLATED DEFECTS

Defect[a]	E_f (eV)
V''_{Pb} (Pb^{2+} vacancy)	19.77
$V^{\cdot}_{F}$ (F^- vacancy)	5.82
$V^{\cdot}_{Cl}$ (Cl^- vacancy)	3.09
$Pb^{\cdot\cdot}_i$ (Pb^{2+} interstitial)	−10.03
F'_i (F^- interstitial)	−1.31
Cl'_i (Cl^- interstitial)	2.93
$F^{\times}_{Cl}$ (F^- on Cl^- site)	−1.69
$Cl^{\cdot}_{F}$ (Cl^- on F^- site)	3.74

[a] The defects are described by Kroger–Vink notation; V and i refer to vacancy and interstitial, respectively. Superscripts indicate the charge of the defect relative to the normal site.

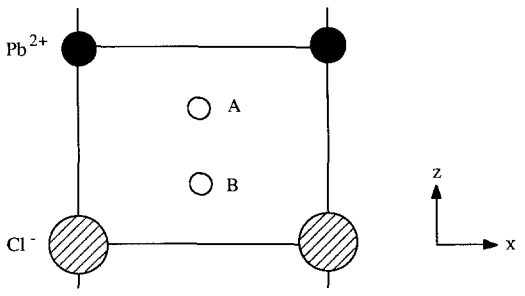

FIG. 1. Stable positions for interstitial ions in the Pb/Cl face after relaxation.

found from simulations of BaFBr, BaFCl, and SrFCl (*20*).

Six types of intrinsic disorder are considered to be feasible for PbFCl, namely, Pb, F, or Cl Frenkel defects, and PbFCl, PbF_2, or $PbCl_2$ Schottky-like defects. The Frenkel defects can be represented by the following reactions:

$$Pb_{Pb} \rightleftarrows V''_{Pb} + Pb_i^{\cdot\cdot} \quad (2)$$

$$F_F \rightleftarrows V_F^{\cdot} + F_i' \quad (3)$$

$$Cl_{Cl} \rightleftarrows V_{Cl}^{\cdot} + Cl_i' \quad (4)$$

and similarly the Schottky defects:

$$Pb_{Pb} + F_F + Cl_{Cl} \rightleftarrows V''_{Pb} + V_F^{\cdot} + V_{Cl}^{\cdot} + PbFCl \quad (5)$$

$$Pb_{Pb} + 2F_F \rightleftarrows V''_{Pb} + 2V_F^{\cdot} + PbF_2 \quad (6)$$

$$Pb_{Pb} + 2Cl_{Cl} \rightleftarrows V''_{Pb} + 2V_{Cl}^{\cdot} + PbCl_2 \quad (7)$$

Thus the entries in Table IV together with appropriate cohesive energies can be combined to obtain estimates of the formation energies of the Frenkel and Schottky-like defects, which are reported in Table V. We find that the Frenkel energies are high and unfavorable, the lowest energy being for the fluorine Frenkel pair. The magnitudes suggest that there will be negligible concentration of interstitial ions in undoped PbFCl. As expected, intrinsic defects associated with the Pb sublattice only are not significant.

An important feature of the results is the confirmation of Schottky-like disorder as intrinsic to the material; in particular, the energies reveal that the defect trio associated with Eq. (7) would predominate, leading to a small deviation from stoichiometry, with an excess of F^-. Therefore, nonstoichiometry could be considered to influence the optical properties of the undoped material, by possibly leading to additional absorption (*1*). Our estimates of the Schottky-like defect energies are subject to some uncertainties owing to the uncertainties in the cohesive energies that must be added. Nonetheless, on comparing our calculated formation energy of 2.43 eV with the values quoted in experimental studies we find good agreement. From single crystal ionic conductivity studies (*8*), the measurements parallel to the *c*-axis have led to a Schottky energy of 2.58 ± 0.48 eV, and similarly from measurements perpendicular to the *c*-axis a value of 2.67 ± 0.48 eV was derived. The agreement between theory and experiment lends support to the crystal potential model for PbFCl. It should be noted, however, that Halff and Schoonman (*7, 8*) proposed that the Schottky disorder consisting of both types of anion would predominate;

TABLE V

CALCULATED FORMATION ENERGIES OF FRENKEL AND SCHOTTKY DISORDER

Defect	ΔH_f (eV)
Frenkel	
$(V''_{Pb}Pb_i^{\cdot\cdot})$	9.75
$(V_F^{\cdot}F_i')$	4.52
$(V_{Cl}^{\cdot}Cl_i')$	6.02
Schottky	
$(V''_{Pb}V_F^{\cdot}V_{Cl}^{\cdot})$	4.73
$(V''_{Pb}2V_F^{\cdot})$	5.27
$(V''_{Pb}2V_{Cl}^{\cdot})$	2.43

i.e., they favor the defect equilibrium associated with Eq. (5), in which there is no overall change in stoichiometry. The calculations indicate that this defect is relatively unfavorable. In addition our results are broadly in line with those of a recent simulation study (*20*) that indicate Schottky-like disorder involving two Br and two Cl vacancies is the most favorable defect in BaFBr and SrFCl.

3.2. *Ion Migration*

Measurements of ionic conductivity in PbFCl (*6–8*) have shown that the anion mobility is high and anisotropic. The latter observation is not surprising in view of the tetragonal layered nature of the crystal structure. The location of ions and available space in the perfect lattice suggests that interstitial diffusion is unlikely. This is indeed confirmed from experiment and our defect calculations, which find the formation of interstitial disorder unfavorable. Hence, ion diffusion in PbFCl is dominated by vacancies.

The possible mechanisms for anion vacancy migration have been examined by Halff and Schoonman (*8*), which are illustrated in Fig. 2, indicating a considerable variety of pathways. Of the seven diffusion mechanisms considered, three involve fluorine vacancies (denoted by F1, F2, and F3), and the other four are concerned with chlorine vacancies (denoted by C1 to C4). Mechanisms F3 and C4 are associated with antisite defect structures that involve, for example, migration of a chlorine ion into a fluorine vacancy. Owing to the number of possible diffusion mechanisms, an unambiguous interpretation of the conductivity data and subsequent assignments can be difficult. Therefore, reliable theoretical values for migration activation energies, which are key factors in the hopping process model, are useful to aid in the analysis of the available experimental data.

Activation energies are calculated from the energy of the saddle-point configuration; that is, the maximum in the energy profile for the migration path relative to the energy of the ground state. This is shown schematically in Fig. 3. Such an energy profile is mapped out by calculating the defect energy of the migrating ion at positions

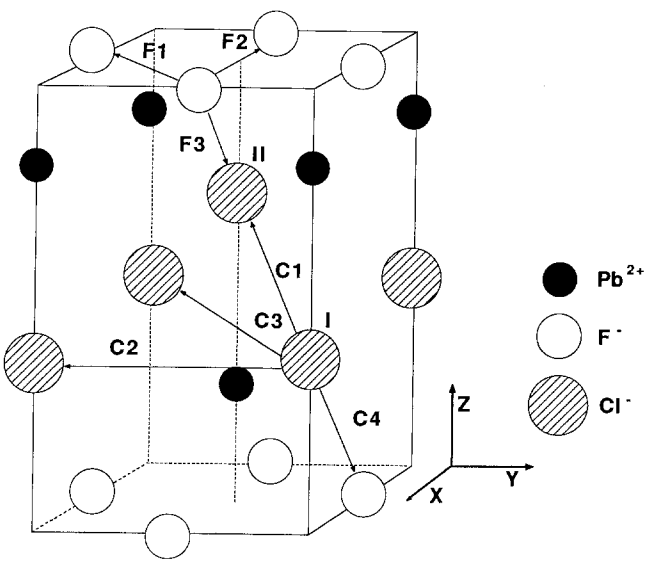

FIG. 2. Crystal structure of PbFCl and possible anion vacancy migration mechanisms (after Ref. (*8*)).

along the diffusion path. This procedure is acceptable provided the hopping model of ion migration is a valid approximation; a topic discussed in detail by Catlow (*31*). In general, the hopping description is acceptable when the activation energy, E_a, satisfies the condition $E_a \gg kT$. This condition holds for most solids, but for the important exception of superionic conductors.

For the anion vacancy mechanism there is a direct path for the migrating ion into an adjacent vacancy. Thus, energy profiles were calculated for each of the seven mechanisms in PbFCl. The resulting profiles confirmed that the maximum energy corresponded to the symmetric configuration, with the migrating ion midway between the two equilibrium positions. The calculated activation energies are reported in Table VI, together with the values derived from ionic conductivity measurements (*8*) of undoped single crystals parallel and perpendicular to the *c*-axis; also indicated are the assignments proposed from the data analysis of Halff and Schoonman (*8*).

TABLE VI

ACTIVATION ENERGIES FOR ANION VACANCY MIGRATION

Mechanism	E^a (eV)	$E_\parallel^b$ (eV)	$E_\perp^c$ (eV)
F vacancy			
F1	0.70		0.66 ± 0.06[d]
F2	2.28		
F3	1.64	1.7 ± 0.1	
Cl vacancy			
C1	0.32	0.29 ± 0.03[d]	
C2	1.58		0.34 ± 0.03[d] 1.55 ± 0.16
C3	5.50		
C4	0.92	0.84 ± 0.06[d]	

[a] Calculated values.

[b,c] Experimental activation energies from measurements parallel and perpendicular to the *c*-axis, respectively.

[d] Assignments proposed by Halff and Schoonman (*8*).

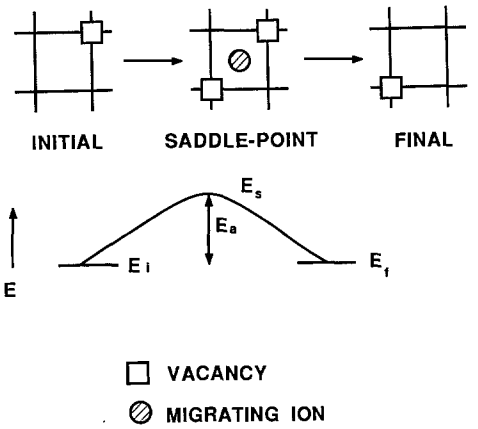

Fig. 3. Schematic representation of an intraplanar vacancy migration mechanism.

For the mechanisms F2 and C3 large interactions between ions in the saddle-point configuration, and hence high energy mechanisms, seem quite reasonable on geometric grounds. This is confirmed by our results which indicate that these two mechanisms are energetically expensive and, therefore, unlikely to contribute to the ionic conductivity. Examination of Table VI shows that the interplanar Cl vacancy migration (C1) clearly emerges as the lowest energy mechanism with an activation energy of 0.32 eV. Our result is in excellent agreement with the observed value of 0.29 eV and confirms that the low temperature conductivity arises from the mobility of Cl vacancies. As expected, interplanar diffusion (C1) is a higher probability process than intraplanar diffusion (C2) since the corresponding Cl–Cl distances involved are 3.624 and 4.106 Å, respectively. The mechanism with the smallest barrier to F vacancy migration is found to be F1 with an activation energy of 0.70 eV. This finding, again, is in good accord with the experimental value of 0.66 eV and suggests that F vacancy conduction will become more important at higher temperatures. Indeed, the transition from Cl to F ion conduction has

been observed in the region of 520–560 K (*6–8*). From the conductivity data Halff and Schoonman (*8*) tentatively assigned the activation energy of 0.84 eV to C4, a mechanism that involves antisite formation. Our computed value of 0.92 eV for C4 provides support for this assignment. In addition, an unassigned energy of 1.7 eV correlates well with a calculated activation energy of 1.64 eV for the antisite mechanism F3. Comparison of the calculated energies with the assignments of Halff and Schoonman reveals, in general, a good measure of agreement.

The result for the intraplanar Cl vacancy mechanism (C2), however, shows a significant discrepancy between theory and experiment: their assignment of $E_\perp$ (0.34 eV) to C2 is over 1 eV smaller than the computed value. The large difference may reflect inadequacies in the short-range potential describing the Cl–Cl interaction. However, in view of the impressive agreement with experiment for the other activation energies and also for the Schottky formation energy, we would be surprised to find discrepancies in the calculations of this magnitude. An alternative possibility is that $E_\perp$ (0.34 eV) is associated with the interplanar mechanism C1; that is, the experimental values of 0.34 and 0.29 eV refer to the same migration mechanism. This result is not surprising since mechanism C1, which involves diagonal zig-zag motion, is likely to have components in both parallel and perpendicular directions to the *c*-axis. Finally, it is interesting to note that the calculated energy of 1.58 eV for mechanism C2 correlates closely with an observed and previously unassigned value of 1.55 eV. Therefore, we conclude that the chlorine vacancy migration mechanisms C1 and C2 are associated with the experimental activation energies of 0.34 and 1.55 eV, respectively.

3.3. V_k Centers

Various hole species have been investigated in connection with the luminescence properties of the alkaline–earth fluorohalide materials (*13, 32*) although the storage phosphor mechanism is still uncertain. Despite the fact that PbFCl has been known for some time, precise structural and energetic information on V_k centers are not available. Our approach to this problem follows closely the previous theoretical treatment of the self-trapped hole, based on the "molecule in the crystal" model; see review by Stoneham (*33*). This model assumes that the electronic properties of the V_k center can be interpreted in terms of an X_2^- molecular ion, with the surrounding crystal lattice affecting the equilibrium bond distance only within the defect molecule.

The potential energy curves between the components of the X_2^- molecular anions have been computed from valence-bond pseudopotential calculations for Cl_2^-, Br_2^-, and I_2^- (*34*), and from self-consistent molecular orbital calculations for F_2^- (*35*). For lattice calculations these potential curves were subsequently fitted to the three-parameter potential function of the analytical form discussed in Section 2 (*36, 37*). The resulting potentials and shell model parameters for Cl_2^- and F_2^- are listed in Table II. With regard to the short-range interactions between the host crystal ions and the V_k ions, these are assumed to be the same as those employed for the perfect lattice. We note that within the V_k center the hole is distributed equally between the two-component ions, so that each ion is assigned a net charge of $-\frac{1}{2}$. It is worth stressing that this general approach has been applied successfully to studies of V_k centers in a variety of halide crystals (*17, 20, 21, 36, 37*).

In the present study we have calculated the formation energy and equilibrium structure of the Cl_2^-, F_2^-, and ClF^- V_k centers. For the Cl_2^- species two configurations were considered: a nearest-neighbor pair in the same plane and a pair in which the two-component ions are in adjacent planes with the shortest possible interatomic spacing.

TABLE VII

V_k DEFECT ENERGIES[a]

Defect	E_D (eV)	E_F (eV)
F_2^-	7.46	11.59
FCl^-	7.21	10.84
Cl_2^- (in-plane)	5.04	8.67
Cl_2^- (out-of-plane)	4.41	8.04

[a] Definitions of E_D and E_F in the text.

We refer to the former as an in-plane V_k and to the latter as an out-of-plane V_k. Note that the angle between the a–b plane and the molecular axis of the out-of-plane V_k is approximately 40°. The V_k relaxation energies, E_D, which correspond to the energy required to remove two X^- ions to infinity and then replacing them with an X_2^- molecule, are presented in Table VII. Estimates of the hole formation energy, E_F, also listed in Table VII, were evaluated by using the appropriate electron affinities of the halogen atom. Thus the V_k defect energies have a consistent reference point within the PbFCl system. We note, however, that these formation energies do not include the defect energy associated with the electron trap usually doped into the material, which would make the energies less endothermic.

Examination of the entries in Table VII reveals that the out-of-plane Cl_2^- species is calculated to be the most favorable V_k center. This result suggests that if a certain degree of hole trapping defects is present, created during X-irradiation, for example, then this V_k center configuration would be the principal product in the nominally pure material. At present there are no corresponding experimental data on PbFCl with which comparisons can be made. Experiments to detect such hole defects in PbFCl, in particular employing spin-resonance techniques, would therefore be of considerable interest. Nevertheless, from ESR measurements (*32*) of the isostructural BaFCl crystal, only the out-of-plane Cl_2^- V_k was observed, which would be consistent with our results. We should add that the Cl_2^- defect in BaFCl is thermally unstable at room temperature; above ~140 K the V_k center decays as the highly mobile hole species is annihilated, possibly by recombination with an F center (*38*) or by dimerization to give Cl_2 or Cl_3^- species (*21*).

In Table VIII we list the separations between the two-component ions of the V_k centers after relaxation, and compare them with the equilibrium bond lengths for both the free molecular anions and the perfect crystal. These distances indicate that the most stable self-trapped hole, the out-of-plane Cl_2^- V_k, is not significantly distorted within the crystal lattice since Tasker *et al.* (*34*) computed a free molecule bond length of 2.71 Å. Indeed, the deviations of $R(V_k)$from R(free X_2^-) for all the configurations considered are small (Table VIII). These results lend support to the X_2^- molecular ion model for the V_k center, with the crystal lattice environment inducing only a slight perturbation of the defect geometry. Previous studies have also confirmed the close similarity between the V_k center and the free X_2^- molecule, with regard to interatomic separations, and corresponding optical and spin resonance parameters (*17, 33, 36, 37*).

When comparing the V_k center separations of the homonuclear molecules with the perfect crystal bond lengths, we find large differences of the order of 1 Å. This clearly demonstrates that substantial relaxations of the V_k component ions are associ-

TABLE VIII

INTERATOMIC SEPARATIONS (IN Å)

Configuration	$R(V_k)$	R(free X_2^-)	R(crystal)
F_2^-	2.03	1.90[a]	2.90
FCl^-	3.22	—	3.26
Cl_2^- (in-plane)	3.00	2.71[b]	4.11
Cl_2^- (out-of-plane)	2.72	2.71[b]	3.63

[a] Reference (*35*).
[b] Reference (*34*).

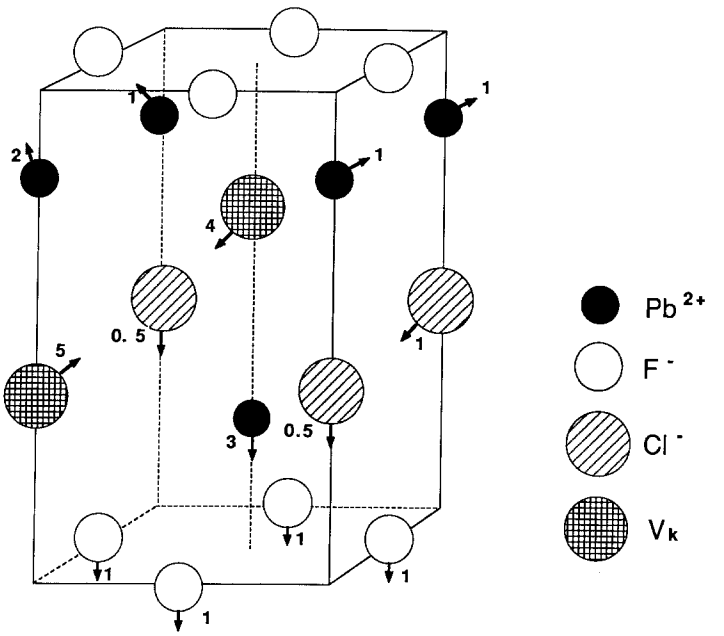

FIG. 4. Relaxation of lattice ions with formation of the out-of-plane Cl_2^- V_k center. Approximate displacements are indicated (in 10^{-1} Å).

ated with the formation of the defect. Figure 4 illustrates schematically the vector displacements of the ions forming and the ions near the out-of-plane Cl_2^- V_k center during the lattice relaxation. The most important movement is that of the V_k center ions, with the $(Cl–Cl)^-$ distance decreasing by ~25% from the perfect lattice positions. In addition the local structure immediately surrounding the V_k center is strongly perturbed: large displacements away from the defect are found for the neighboring Pb ions. Note that the adjacent F and Cl ions also move away but by a smaller degree. Careful examination of the relaxed positions indicates that the lattice distortion diminishes with the distance from the defect. As remarked earlier, no experimental data on ion positions are available; such information could be derived from ENDOR studies and would be useful in assessing the sensitivity of the pair-potentials employed.

4. Conclusions

Three important features have emerged from our study of PbFCl that are generally in line with the properties of other mixed fluorohalide systems. First, the calculations have shown Schottky-like disorder involving Pb and Cl vacancies to be energetically favorable and suggest a small deviation from the stoichiometric composition. Vacancies rather than interstitials are, therefore, predicted to be the predominant intrinsic point defects, in accord with experiment. Second, the results confirm that the low temperature conductivity region is attributed to the migration of Cl vacancies via an interplanar mechanism. The agreement between computed and experimental activation energies clearly shows the value of the methods in quantitatively simulating defect processes. Indeed, our discussion has led to a reinterpretation of

the observed migration activation energy of 0.34 eV which, we believe, should be assigned to the interplanar mechanism C1. Finally, the out-of-plane Cl_2^- V_k center is predicted to be the most stable self-trapped hole species and could, therefore, play a vital role in the mechanism of photostimulated luminescence.

Acknowledgments

I am grateful to R. C. Baetzold and R. S. Eachus for many helpful discussions.

References

1. A. J. H. Eijkelenkamp, *Phys. Status Solidi A* **76,** 153 (1976).
2. A. J. H. Eijkelenkamp, *Solid State Commun.* **19,** 295 (1976).
3. A. J. H. Eijkelenkamp, *J. Solid State Chem.* **7,** 313 (1976).
4. K. Somaiah and S. R. Moinuddin, *J. Mater. Sci. Lett.* **6,** 417 (1987).
5. A. F. Halff and J. Schoonman, *Phys. Status Solidi A* **40,** 511 (1977).
6. J. Schoonman, G. J. Dirksen, and G. Blasse, *J. Solid State Chem.* **7,** 245 (1973).
7. A. F. Halff and J. Schoonman, *Z. Phys. Chem.* **109,** 161 (1978).
8. A. F. Halff and J. Schoonman, *J. Solid State Chem.* **27,** 397 (1979).
9. N. N. Greenwood, "Ionic Crystals, Lattice Defects and Non-stoichiometry," Butterworths, London (1970).
10. W. Nieuwenkamp and J. M. Bijvoet, *Z. Kristallogr.* **81,** 469 (1932).
11. J. Hölsä, M. Leskelä, and L. Niinistö, *J. Solid State Chem.* **37,** 267 (1981).
12. J. L. Sommerdijk, J. M. P. Verstegen, and A. Bril, *J. Lumin.* **8,** 502 (1974).
13. R. V. Bauer, J. R. Niklas, and J. M. Spaeth, *Phys. Status Solidi B* **118,** 557 (1983).
14. K. Takahashi and J. Miyahara, *J. Electrochem. Soc.* **132,** 1492 (1984).
15. C. R. A. Catlow, J. Corish, K. M. Diller, P. W. M. Jacobs, and M. J. Norgett, *J. Phys. (Paris) Colloq.* **37,** C7–253 (1976).
16. W. C. Mackrodt and R. F. Stewart, *J. Phys. C* **12,** 431 (1979).
17. P. E. Cade, A. M. Stoneham, and P. W. Tasker, *Phys. Rev. B* **30,** 4621 (1984).
18. C. R. A. Catlow, M. J. Norgett, and T. A. Ross, *J. Phys. C* **10,** 1627 (1977).
19. P. J. Bendall, C. R. A. Catlow, and B. E. F. Fender, *J. Phys. C* **14,** 4377 (1981).
20. R. C. Baetzold, *Phys. Rev. B* **36,** 9182 (1987).
21. R. C. Baetzold, *J. Phys. Chem. Solids* **50,** 915 (1989).
22. M. J. Norgett, AERE Harwell Report R37650 (1974).
23. M. Leslie, SERC Daresbury Lab. Report DL/SCI/TM31T (1982).
24. C. R. A. Catlow and W. C. Mackrodt (Eds.), "Computer Simulation of Solids," Lecture Notes in Physics, Vol. 166, Springer-Verlag, Berlin (1982).
25. F. Agullo-Lopez, C. R. A. Catlow, and P. D. Townsend, "Point Defects in Materials," Chap. 11, Academic Press, London (1988).
26. B. G. Dick and A. W. Overhauser, *Phys. Rev.* **112,** 90 (1958).
27. J. H. Harding, *Cryst. Lattice Defects Amorphous Mater.* **15,** 71 (1987).
28. R. G. Gordon and Y. S. Kim, *J. Chem. Phys.* **56,** 3122 (1972).
29. A. M. Stoneham and J. H. Harding, *Ann. Rev. Phys. Chem.* **53,** 80 (1986).
30. K. R. Balasubramaian, T. M. Haridasan, and N. Krishnamurthy, *Chem. Phys. Lett.* **67,** 530 (1979).
31. C. R. A. Catlow, *Solid State Ionics* **8,** 89 (1983).
32. M. Yuste, L. Taurel, and M. Rahmani, *Solid State Commun.* **17,** 1435 (1975).
33. A. M. Stoneham, "Theory of Defects in Solids," Chap. 18, Oxford Univ. Press, London (1975).
34. P. W. Tasker, G. G. Balint-Kurti, and R. N. Dixon, *Mol. Phys.* **32,** 1651 (1976).
35. T. L. Gilbert and A. C. Wahl, *J. Chem. Phys.* **55,** 5247 (1971).
36. R. Monnier, K. S. Song, and A. M. Stoneham, *J. Phys. C* **10,** 4441 (1977).
37. M. J. Norgett and A. M. Stoneham, *J. Phys. C* **6,** 229 (1973).
38. R. S. Eachus, personal communication.